International Journal of Innovation in Mechanical Engineering and Advanced Materials
Homepage: publikasi.mercubuana.ac.id/index.php/ijimeam
Vol. 8 (No. 1), 2026, pp. 12-25
DOI: 10.22441/ijimeam.v8i1.35039

Article

Numerical Study of Nano Enhanced PCM Incorporated Heat Sink with Wavy Shaped Plate Fins

Soumik Kumar Hazra *

Department of Mechatronics Engineering, Faculty of Engineering, University of Debrecen, Otemeto Utca 2-4, Debrecen 4028, Hungary
*Corresponding Author: soumikhazra4390@mailbox.unideb.hu (SKH)

Abstract

Modern high-power electronic devices require efficient passive cooling strategies to maintain safe operating temperatures. This study presents a two-dimensional numerical investigation of a nano-enhanced phase change material (NePCM)-based heat sink incorporating wavy-shaped plate fins. The NePCM consists of paraffin with 3 wt% CuO nanoparticles to enhance thermal conductivity. The novelty of this work lies in the integration of wavy-shaped fins to promote natural convection and accelerate PCM melting, thereby improving heat dissipation performance. The governing continuity, momentum, and energy equations are solved using the enthalpy–porosity method under a constant heat flux of 10,000 W/m^2 and a convective boundary condition of 10 W·m^{-2}·K^{-1}. Parametric analyses are conducted by varying the number of cavities (3, 5, and 7) and fin height (40–50 mm). The results show that the NePCM heat sink reduces the peak temperature from 438 K (conventional) to 381 K, corresponding to a reduction of approximately 13% after 30 minutes. The wavy fin configuration enhances fluid circulation within the molten PCM, leading to faster melting and improved heat absorption. Increasing cavity number from 3 to 7 reduces the average temperature by up to ~7 K, while increasing fin height to 50 mm further lowers the temperature by approximately 10–20 K compared to shorter fins. The combined effect of latent heat storage and enhanced natural convection induced by wavy fins significantly improves thermal management performance, making the proposed design a promising solution for compact electronic cooling applications.

Article Info:
Received: 8 July 2025
Revised: 4 April 2026
Accepted: 5 April 2026
Available online: 7 April 2026

Keywords:
PCM; NePCM; temperature; heat sink; liquid fraction; cavity

© 2026 The Author(s). Published by Universitas Mercu Buana (Indonesia). This is an open-access article under *CC BY-SA* License.

1. Introduction

The miniaturization and development of newer power intensive processors, integrated circuits, MOSFETs and LED lights has led to the need to maintain these devices at their optimum operating temperature. Resultant increase in the heat flux greatly reduces the capabilities and life of the electronics [1]-[2]. Hence, continuous efforts are being made to provide them with optimal cooling performance to ensure better performance and longer operational life. The conventional method of passive cooling of these electronic components by natural convection from heat sinks and heat pipes have been deemed insufficient owing to large heat load [3].

Existing cooling systems are usually active coolers, incorporating forced convection inducing fans and circulation pumps [4]–[8]. Recently there has been emergence of thermoelectric coolers operating using Peltier effect [9]. But both the types of cooling devices use external power and are often cumbersome. Moving parts give rise to vibrations and undesirable noise and are maintenance intensive. For the afore-mentioned drawbacks the need for the development of better performing cooling systems. In this quest Phase Change Material (PCM) incorporating heat sinks can be instrumental in addressing the challenge of maintaining electronics devices and components at their optimal temperature. The high latent heat of fusion of PCMs has promoted it amongst researches to be used in electronics cooling apparatuses [10]-[14]. PCM was first introduced as coolant in electronics by NASA for the robotic arm of spacecrafts [15]-[17]. PCMs absorb and hold high amounts of latent heat during melting and releases it back on freezing. This absorption of high latent heat can become instrumental in developing better heat sinks with ability to vent off heat at a faster rate. Phase

How to cite:

S. K. Hazra, "Numerical study of nano enhanced PCM incorporated heat sink with wavy shaped plate fins," *Int. J. Innov. Mech. Eng. Adv. Mater*, vol. 8, no. 1, pp. 12-25, 2026

Change Materials (PCM) inherently also have high specific heat, high stability after repeated charging and discharging cycles. The afore mentioned properties contribute to maximized heat storage, low expansion on heating, repeated use over a long duration of time and predictable freezing behavior owing to the property of thermal stability even after numerous cycles of melting and freezing. With also these positive qualities suffers from low thermal conductivity, hindering faster heat conduction.

To address this problem, two types of approaches have been undertaken. One is using Thermal Conductivity Enhancing structures (TCE) and by addition of nanoparticles to pure PCM. Baby et al. compared heat sinks having pin and plate fins with and without PCM [18]. Results showed that the finned heat sink incorporating PCM performs better than the one without PCM and fin. Heat sinks with PCM filled cavities were experimented with by Kalbasi et al. [19]. Results revealed that fins aided in the melting of PCM. Bhuyian et al. from his study on various shapes of cavities of heat sinks concluded that the cavity with maximum PCM holding capacity performs the best [20]. It is applicable for enclosed parts with lower convection rate. Plates finned heat sink was studied by Deng et al. varying in pitch and cavity thickness [21]. More fins lead to increased thermal performance and ability to operate longer. Heat sink with fins extending above the PCM led to more natural convection and longer operation time [22]. In a similar study by Bayat et al. found out that heat sinks with plate fin and PCM are more responsive to change sin heat flux coming from electronic components [23]. In other methods to improve thermal conductivity of PCM nanoparticles are added. Vitorino et al. added 10% graphite to paraffin wax to achieve better thermal conductivity [24]. Similarly other nanoparticles of CuO, silver, Sci-Si_3N_4, were used by various researchers [25]-[29].

The numerical study of novel PCM containing heat sink was envisioned and pioneered by and numerically presented by Shatikian et al. [30]-[31]. The formulation attempted to calculate the unsteady velocity and temperature inside the domain by solving the conservation equations of energy, continuity, and momentum. This has since been a standard approach for numerical simulations.

In recent years, several studies have reported the application of PCM based heat sink to address the problem of overheating in electronic devices. In these studies, PCM have been placed inside the heat sink in varied quantities [18]-[20]. PCM is either enclosed within the heat sink or kept in open cavities, built in the heat sink. Balaji et al. experimentally studied constant heat input with intermittent heat load applied to PCM based heat sink and the results showed that size of PCM based heat sink under intermittent load is smaller than that of under continuous heat [2]. Signifying need for increased cavity size. Ramesh et al. proposed the development of a heat sink for the LED array cooling using heat sink with PCM and concluded that 10mm or more cavity width increases the melting rate of PCM in the heat sinks [3]. Kalbasi et al. proposed a hybrid heat sink with air and PCM in alternate cavities of the heat sink to increase natural convective heat transfer. With a convective heat transfer coefficient (h) equal to $10Wm{-}2K{-}1$, natural convection performs better than forced convection (higher value of h). Ambient temperature plays an important role in PCM's ability to absorb and store thermal energy in case of forced convection system; hence natural convection is places with everchanging ambient temperature [4]. Heat sink with PCM has better cooling efficiency for longer usage under both free and forced convection system whereas the heat sink with nano PCM is preferable for intermittent and temporary usage [4]. Nazir et al. compared different PCM for energy storage based on thermo-physical properties like melting point, thermal energy storage density. The results showed that for enhancing PCM qualities and properties, encapsulation and using nanomaterial additives are the two best ways because protection from environment, corrosion, and energy storage compatibility can be achieved by these two methods [5].

Mozafari et al. experimented using both single and multiple PCM heat sink for electronic device cooling revealing that multiple n-eicosane based heat sink has better operational performance than single n-eicosane based heat sink for prolonged operational hours by 4%-12% [6]. Farzanehnia et al. investigated the thermal management of nano-PCM heat sink and found that chipset's peak temperature increases while operating at constant power [7]. Mahmoud et al. studied PCM based heat sink behavior during charging and discharging process using different fin-types. It was found that the parallel rectangular plate fin arrangement with six cavities performed better in charging process by absorbing more heat but in contrast the honeycomb patterned heat sink exhibited more efficient discharging with a short heat rejection time [8]. Hence shapes close to the honeycomb pattern are expected to exhibit improved discharging property. Kozak et al. performed a comparison of PCM filled heat sink and hybrid heat sink from which the paper was concluding that under high power load, PCM based heat sink performs better [9]. Hosseinizadeh et al. studied the application of a PCM-based heat

sink for cooling computer chipset, revealing that increasing the number of fins and fin height results in a significant increase in overall thermal performance whereas increasing the fin thickness only leads to negligible improvement in thermal performance. There is a critical fin thickness equal to 4 mm and beyond this opting for a thicker fin will not lead to further improvement of thermal performance [10]. For identical geometries, both the Nusselt number and the melt fraction are governed by the combined effect of the Fourier and Stefan numbers [3].

Despite extensive research on PCM-based heat sinks, the role of fin geometry in enhancing natural convection within PCM domains remains insufficiently explored. Most existing studies have primarily focused on straight or rectangular fins, which mainly improve heat conduction but induce limited flow disturbance and weak convective mixing. In contrast, wavy-shaped fins introduce periodic geometric perturbations that can intensify buoyancy-driven flow, disrupt thermal boundary layers, and promote more effective thermal mixing, thereby accelerating PCM melting kinetics. Nevertheless, the specific impact of wavy fin geometry on the thermal performance of nano-enhanced PCM (NePCM) systems has not been systematically investigated. From the literature survey it can be identified that heat sinks containing PCM can outperform conventional heat sinks in heat removal performance. Natural convection is more advantageous than forced convection being free of external power need, scalable and requiring least maintenance. The shape and arrangement order of the cavities influence the thermal performance, while the nanoparticle addition enhances the thermal conductivity of the PCM. The proposed system can respond to both constant and intermittent heat loads.

The present study aims to overcome the limitations of existing electronic cooling systems by solving the governing continuity, momentum, and energy equations associated with PCM melting. In this model, the effects of PCM expansion, convection within the fluid phase (including melted PCM and air), and solid-phase motion in the liquid are neglected [16]. A similar modeling approach has been successfully applied in previous studies, particularly by Shatikian et al., who conducted a numerical investigation of PCM melting and solidification in a heat sink with vertical plate fins [30]. Details of transiting temperature and phase is obtained as functions of time, showing evolving melt fraction of the PCM. In the current numerical study, the approach is of a parametric investigation of melting in a compact heat sink, with a nano-enhanced PCM stored between the fins. Based on this the best performing heat sink is numerically studied to find the best suited cavity height for practical use. The heat sink is tested for extracting heat from an electronic component working at constant power [32]-[41]. The shapes of the fins considered in this study are wavy. These cavities between the fins are filled with paraffin nano enhanced with copper oxide (CuO) nano particles.

Despite extensive studies on PCM-based heat sinks, limited attention has been given to the role of fin geometry in enhancing natural convection within PCM domains. Most previous studies have focused on straight or rectangular fins, which primarily enhance conduction but provide limited flow disturbance. The use of wavy-shaped fins introduces periodic geometric perturbations that can intensify buoyancy-driven flow, disrupt thermal boundary layers, and accelerate melting kinetics. However, the influence of such wavy geometries on NePCM performance remains insufficiently explored. Therefore, the objective of this study is to investigate the thermal performance of a NePCM-based heat sink incorporating wavy plate fins, with particular emphasis on how wavy geometry influences melting behavior, natural convection, and temperature reduction. The effects of cavity number and fin height are also examined to identify optimal design configurations.

2. Methods

2.1. Problem description

A processor cooling unit with wavy shaped plate fins has been shown in Figure 1 showing the length (L), width (W) and height (H). The value of length (L) and width (W) equals to 120mm and 120mm respectively, as shown on Table 1 and Figure 1. Constant heat flux is applied from the bottom of the plate. The cavity between the fins is filled with Phase Change material. The PCM used in this present study is paraffin and CuO nanoparticles have been dispersed as thermal conductive enhancers. Considering heat will only flow in the x, y direction, two-dimensional domain has been taken.

Figure 2(b) labels the two-dimensional computational domain by a length (L), height of fins (HF), thickness of fins (TF), thickness of cavities (TC), thickness of bottom plate (TP) and amplitude of wavy fins (A).

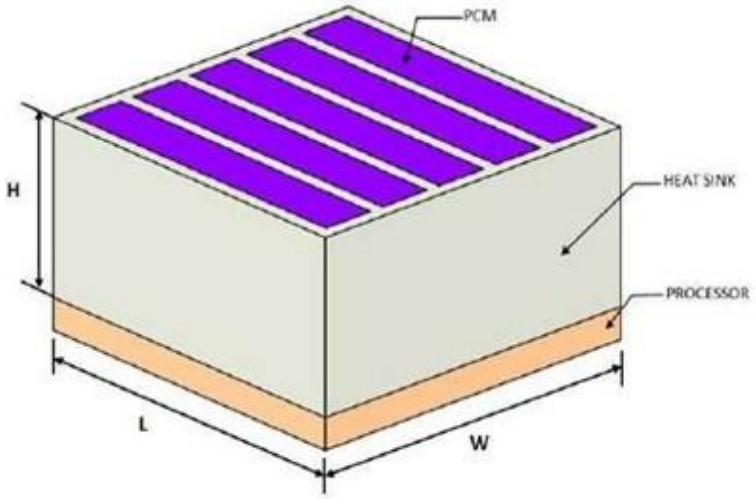


Figure 1. Isometric view of processor cooling unit.

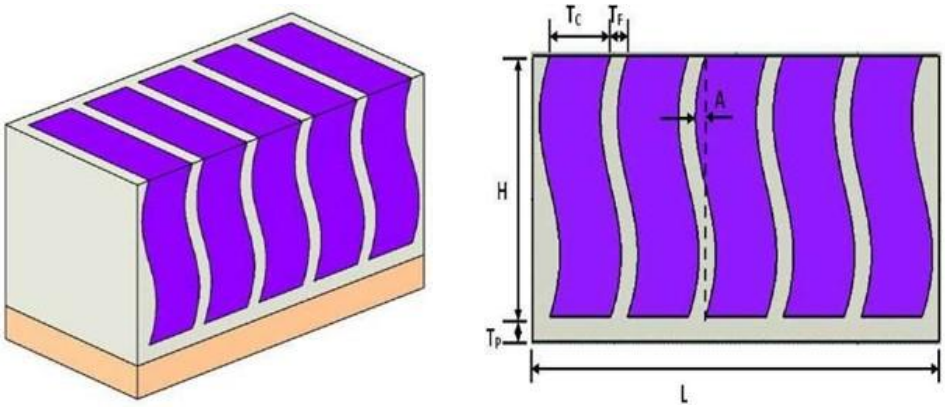
Table 1. Dimensions of the heat sinks with different number of cavities.

Number of Cavity	Total Width of Cavity	Width of each cavity (W_c) (mm)	Number of Fins	Width of each Fins (W_t) (mm)
3	90	30	4	7.5
5	90	18	6	5
7	90	12.857	8	3.75

In this study, the thickness of the bottom plate (T_p) and the amplitude of the wavy fins (A) are taken as 5 mm and 1 mm respectively, as shown in Figure 2. Firstly, a comparison has been made between a conventional heat sink and a heat sink with nano- enhanced PCM enclosed between the wavy plate fins. To identify the optimal geometry of the nano-enhanced PCM filled heat sink the number of PCM filled cavities (N) has been varied keeping the volume of the PCM constant. So, the thickness of the fins is also changed accordingly. Table 1 represents the dimensions of the heat sinks with different number of cavities. The height of fins (HF) has also been varied to 40mm, 45 mm and 50 mm height. The %wt composition of CuO dispersed in paraffin is taken as 3% in this study [25].

2.2. Governing equation and boundary conditions of mathematical modelling

In this study, the transient phase change of PCM is modeled as a two-dimensional, laminar, and incompressible flow. The buoyancy effects are incorporated using the Boussinesq approximation, while volumetric expansion during the phase change process is neglected. The melting process is simulated using the enthalpy–porosity method, in which the mushy zone is treated as a porous medium whose porosity is defined by the liquid fraction of PCM.



(a) (b)

Figure 2. Processor cooling unit; (a) Side view (b) Cross-sectional view.

Consequently, the porosity varies continuously from 0 (solid phase) to 1 (fully liquid phase) during the phase transition. Based on these assumptions, the governing mathematical model is formulated as follows.
The continuity equation:

$$\frac{\partial \rho}{\partial t}+\frac{\partial(\rho u)}{\partial x}+\frac{\partial(\rho v)}{\partial y}=0 \tag{1}$$

The momentum equation:

$$\frac{\partial(\rho u)}{\partial t}+\frac{\partial(\rho u u)}{\partial x}+\frac{\partial(\rho u v)}{\partial y}=-\frac{\partial P}{\partial x}+\frac{\partial}{\partial x}\left(\mu\frac{\partial u}{\partial x}\right)+\frac{\partial}{\partial y}\left(\mu\frac{\partial u}{\partial y}\right)+F_x \tag{2}$$

$$\frac{\partial(\rho u)}{\partial t}+\frac{\partial(\rho u v)}{\partial x}+\frac{\partial(\rho u v)}{\partial y}=-\frac{\partial P}{\partial y}+\frac{\partial}{\partial x}\left(\mu\frac{\partial v}{\partial x}\right)+\frac{\partial}{\partial y}\left(\mu\frac{\partial v}{\partial y}\right)+\rho g\beta\left(T-T_{ref}\right)+F_y \tag{3}$$

The energy equation:

$$\frac{\partial(\rho H)}{\partial t}+\frac{\partial(\rho u H)}{\partial x}+\frac{\partial(\rho v H)}{\partial y}=\frac{\partial}{\partial x}\left(\alpha\frac{\partial T}{\partial x}\right)+\frac{\partial}{\partial y}\left(\alpha\frac{\partial T}{\partial y}\right) \tag{4}$$

where ρ denotes the density of the PCM (kg/m^3), and u and v represent the superficial velocity components in the x- and y-directions (m/s), respectively. The parameter μ is the dynamic viscosity, P is the pressure, and g is the gravitational acceleration. The temperature is denoted by T, while T_{ref} represents the reference temperature, taken as 30 °C in this study, corresponding to the average melting temperature of the PCM. The thermal expansion coefficient is given by β, and the thermal diffusivity is defined as $\alpha=\frac{k}{\rho c_p}$. The terms F_x and F_y represent source terms in the momentum equations, and H denotes the total enthalpy of the PCM.

The source terms F_x and F_y in the momentum equations correspond to Darcy-law-based damping terms that account for the influence of phase change on fluid flow. Here, the subscript x indicates the horizontal direction, while y denotes the vertical direction. These terms are expressed as follows:

$$F_x=-\frac{(1-\xi)^2}{\xi^3+\varepsilon}A_{mush}u \tag{5}$$

$$F_y=-\frac{(1-\xi)^2}{\xi^3+\varepsilon}A_{mush}v \tag{6}$$

where A represents the mushy zone constant, taken as 5×10^6, and $\varepsilon=0.001$ is a small numerical parameter introduced to avoid division by zero when the liquid fraction $\xi=0$. The parameter ξ denotes the melt fraction of the PCM.

The melt fraction ξ is determined based on the temperature distribution, as expressed in Equation (7):

$$\xi=\begin{cases}0\ if\ T\le T_s\\ \dfrac{T-T_s}{T_l-T_s}\ if\ T_s<T\le T_l\\ 1\ if\ T>T_l\end{cases} \tag{7}$$

The total enthalpy of the PCM (H) is calculated as the sum of sensible enthalpy (h) and latent heat contribution (L), as given in Equation (8):

$$H=h+\Delta H=h+\xi L \tag{8}$$

The sensible enthalpy is defined by:

$$h=h_{ref}+\int_{T_{ref}}^{T}C\rho dT \tag{9}$$

In the current numerical simulation, the boundary conditions applied to the domain under study are described as follows. A constant heat flux of 10,000 W/m^2 is applied to bottom of the PCM-filled heat sink is given in Equation. (10).

$$-k\frac{\partial T}{\partial y}|_{y=0} = q \tag{10}$$

Meanwhile, the side walls and the top boundary of the heat sink are subjected to natural convection. The convective heat transfer coefficient and ambient temperature are taken as 10 $W.m^{-2}.K^{-1}$ and 300 K, respectively. The convective heat transfer at these boundaries is expressed as:

$$-k\frac{\partial T}{\partial n} = h(T - T_{amb}) \tag{11}$$

where T_{amb} is the ambient temperature.

Coupled boundary conditions has been applied at the interface between fin and PCM surfaces which is defined as:

$$-K_{fin}\frac{\partial T_{fin}}{\partial \mathrm{n}} = -K_{PCM}\frac{\partial T_{PCM}}{\partial \mathrm{n}} \tag{12}$$

$$T_{fin} = T_{PCM} \tag{13}$$

where *n* is the normal vector of interfaces.

No-slip condition is assumed at the walls and is given as:

$$u = 0, v = 0 \tag{14}$$

2.3. Numerical methods

The numerical simulation employs two-dimensional continuity, momentum, and energy equations to model the behavior of the PCM, along with the energy equation for the solid walls. The heat sink is constructed from copper. A nano-enhanced phase change material (NePCM) is incorporated into the computational domain as a thermal energy storage medium, assuming constant thermophysical properties, including thermal conductivity (k), density (ρ), and viscosity (μ). The material properties of copper and the temperature-dependent thermophysical properties of the NePCM are summarized in Table 2.

The boundary conditions applied to the heat sink for the current study of the different cavities remain same for all the cases, as shown in Table 2. The heat sink is placed over an electronic component producing constant heat flux applied at the base of the heat sink. Nano enhanced PCM (Paraffin wax with 3% CuO nanoparticles) is used as the heat absorbing material with the objective of maintaining the optimum operating temperature of electronic component by removing the heat flux. Initially, the NePCM and the heat sink are at a temperature T_{in} equal to 300 K. At the solid-fluid interface, no slip conditions with same temperature and conductive flux at the solid-fluid interfaces have been applied.

The governing equations, together with the specified boundary conditions, were solved using the ANSYS Fluent 16 solver based on the finite volume method. The pressure–velocity coupling was handled using the SIMPLE algorithm, while the PRESTO scheme was employed for pressure interpolation. A third-order upwind MUSCL scheme was selected for the discretization of both momentum and energy equations to enhance solution accuracy. Under-relaxation factors of 0.9, 0.3, 0.7, and 1.0 were applied for density, pressure, velocity, and temperature, respectively. Convergence of the numerical solution was ensured by setting residual criteria of 10^{-6} for momentum equations and 10^{-9} for the energy equation.

Table 2. Thermo-physical properties of Nano-Enhanced PCM and Copper.

Properties	NePCM	Copper
Density (kg/m^3)	1033.6	8978
Viscosity (Pa.s)	0.0470	
Latent heat (KJ/Kg)	115.28	
Thermal conductivity (W/m.K)	0.576	387.6
Specific Heat (J/Kg.K)	2408.34	381
Thermal expansion coefficient	0.00962	
Solidus temperature (K)	331	
Liquidous temperature (K)	335	

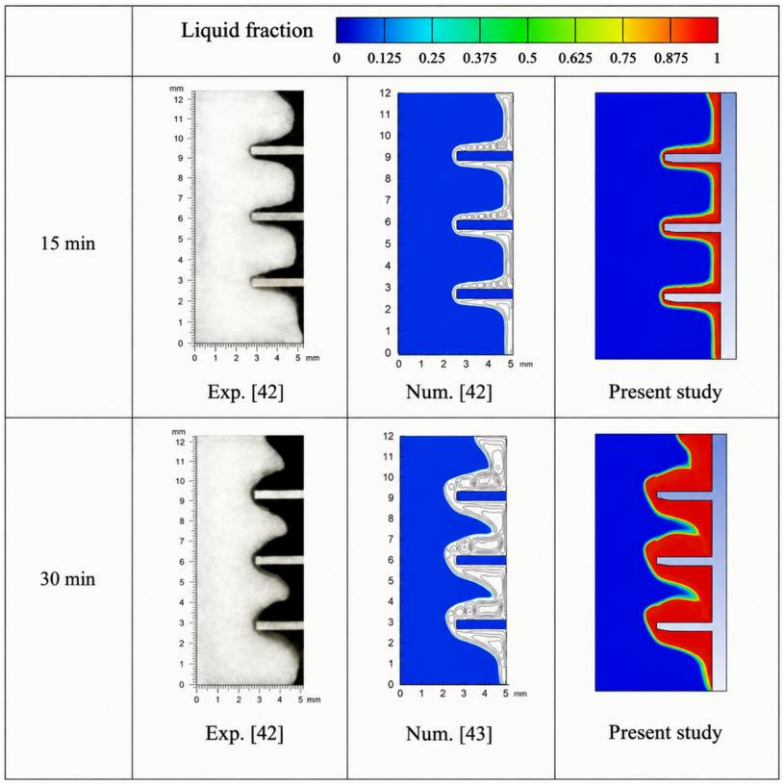


Figure 3. Validation of liquid fraction contours in the three-fin enclosure with prior experimental and numerical investigations [42,43].

Three different grid sizes equal to 600×275, 240×110, and 120×55 were chosen for performing the grid independence test for the computational domain. The time step size for the computation was chosen to be equal to 0.1 sec [1]. The simulations were conducted using double-precision calculations with parallel processing on 20 processor cores, utilizing a workstation equipped with an Intel Xeon Silver CPU operating at 2.5 GHz and 64 GB of RAM.

2.4. Validation

For validation purposes, the present numerical results for PCM melting in a finned enclosure are compared with experimental data reported by Kamkari et al. and numerical results from Karami et al., as illustrated in Figure 3 [42], [43]. The computational domain consists of an enclosure with dimensions of 120 mm in length and 50 mm in height. The aluminum base supporting the fins has a thickness of 5 mm, while the three horizontal fins each have a length of 25 mm and a thickness of 4 mm. The base of the fin located at the right boundary of the enclosure is maintained at a constant temperature of 333 K, whereas all other walls are assumed to be thermally insulated. The PCM is initially at 300 °K. These studies used lauric acid (99% pure) as phase change material with melting temperatures ranging between 43.5-48.2 °C. The results reveal that the simulations of PCM melting in a vertical rectangular enclosure heated from a sidewall closely agrees with prior experimental and computational results.

2.5. Mesh independency test

In the mesh independency study, 1 mm, 0.5 mm, and 0.2 mm element sizes corresponding to grids (120 × 55), (290 × 110) and (600 × 275) are used as shown in Table 3.

Table 3. Mesh independence test parameters.

Grid	No. of elements
240×110	26,400
600×275	165,000
120×55	6,600

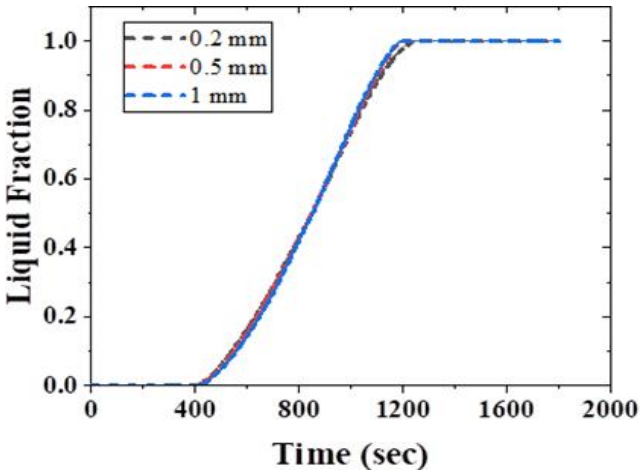


Figure 4. Mesh independency test for 5 cavity heat sinks with PCM enclosed between wavy shaped fins.

The graph in Figure 4 shows the variations in liquid fraction and temperature with respect to time for three different grid sizes. In the graph the plots for respective grids nearly overlapped. Therefore, to make calculations easier and faster the grid size of (290 × 110) with total elements equal to 26,400 is selected for numerical investigation.

3. Results and Discussion

The simulation results provide a comprehensive insight into the thermal performance of wavy finned heat sinks filled with nano-enhanced phase change materials (NePCM) compared to conventional designs. A detailed thermal analysis revealed that the incorporation of paraffin-based NePCM with CuO nanoparticles significantly enhances heat dissipation due to the synergistic effects of latent heat absorption and improved thermal conductivity. Comparative studies show that while the conventional heat sink reaches temperatures as high as 438 K after 30 minutes of operation, the NePCM-based counterpart maintains much lower temperatures, around 381 K, under identical conditions. This substantial temperature reduction is attributed to the latent heat storage capacity of PCM, which effectively delays temperature rise by absorbing thermal energy during the melting process.

Furthermore, varying the number of cavities within the heat sink structure while keeping the total volume of PCM constant demonstrates that increasing the number of cavities (from 3 to 7) markedly improves thermal performance. This is due to the increase in contact area between the PCM and fins, which accelerates the melting process and allows for more efficient thermal regulation. Among the configurations tested, the 7-cavity heat sink outperformed others, reaching a lower peak temperature and achieving a higher melt fraction over the same time span.

Additionally, increasing the fin height from 40 mm to 50 mm further improves thermal performance, offering larger PCM volumes and extended contact surfaces for heat absorption. The 50 mm-high configurations exhibited the lowest temperatures throughout the simulation, validating the design's superior capacity for thermal storage and dissipation. These findings conclusively demonstrate that geometry optimization—through cavity count and fin height—plays a critical role in maximizing the effectiveness of NePCM-integrated heat sinks, positioning them as a robust solution for thermal management in compact, high-power electronic systems.

3.1. Comparison between heat sinks with and without nano-enhanced PCM

To study the effect of using nano-enhanced PCM in the heat sink, a comparison has been drawn between heat sinks, one conventional heat sink and another with nano-enhanced PCM enclosed between the wavy plate fins. After a duration of 15 min and 30 min heat sink temperature is compared. Figure 5 shows the temperature contours of the heat sinks after 15 min and 30 min. From the results, the conventional heat sink has reached to an average temperature of 398.6 K (125.44^{o} C) and 438.02 K (164.86^{o} C) after 15 min and 30 min respectively. The bottom wall temperature of the heat sink was 399.88 K (126.72^{o} C) after 15 min and 439.37 K (166.21^{o} C) after 30 min. Conversely, the sink with NePCM at a similar duration

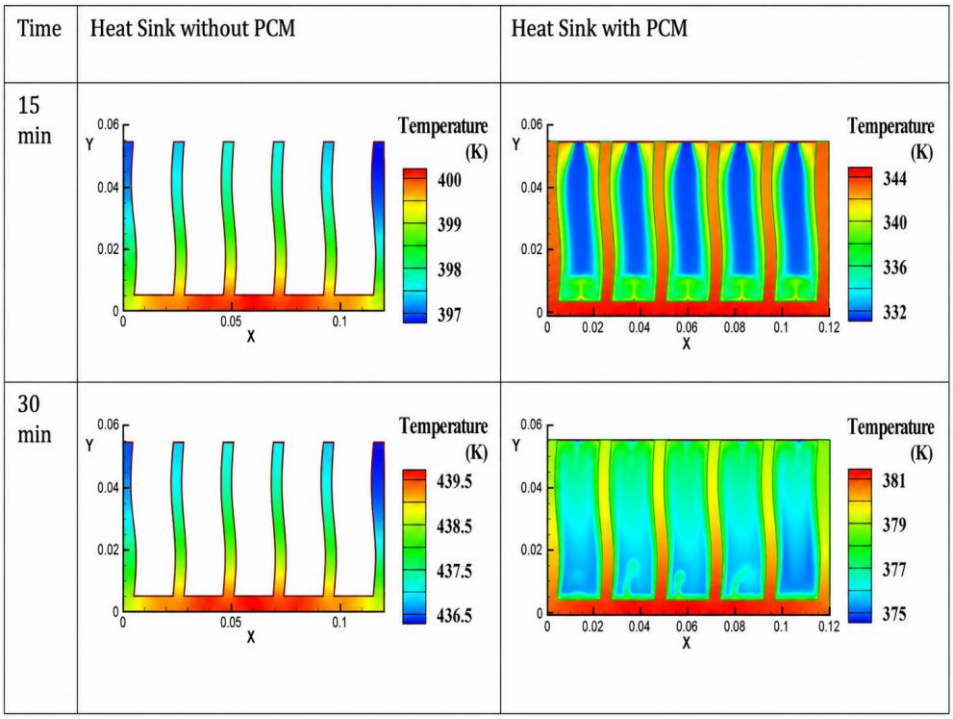


Figure 5. Comparison between Conventional and nano-enhanced PCM heat sinks.

of 15 min and 30 min is seen to attain an average temperature of 343.67 K (70.51° C) and 381.079 K (107.9° C) respectively. The bottom wall temperature of the heat sink was 344.58 K (71.42° C) and 382.17 K (109.01° C) respectively after 15 min and 30 min. Figure 6 shows the temperature variation with time in the heat sinks.

From the graph, it can be easily identified that the use of PCM in between the fins are more effective to keep the system cool. The variation in the bottom wall temperature and average temperature attained by the conventional and NePCM incorporated heat sink can be attributed to the presence of PCM that absorbs heat energy and stores it in form of latent heat. In conventional heat sinks the heat transfer solely depends on the natural convection. But, in case of PCM filled heat sinks the combined effect of natural convection and heat absorption by the PCM performs the task of cooling down the heat sink. A significant part of the heat flux coming from the base of the heat sink gets expended in melting the PCM. This phenomenon compliments the natural convention. Resultantly, temperature rise in the PCM filled heat sink is much lower, which makes it a better solution for heat dissipation challenges, by distribution of heat to the upper regions of the heat sink and maintaining a better thermal potential difference towards the base of the heat sink.

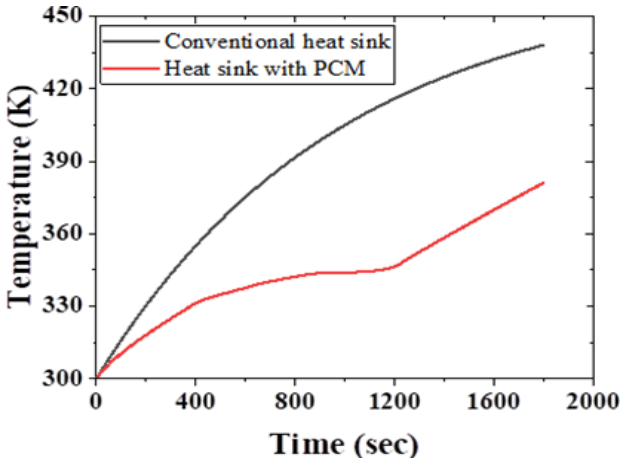


Figure 6. Temperature vs time curve of Conventional heat sink and Heat sink with PCM.

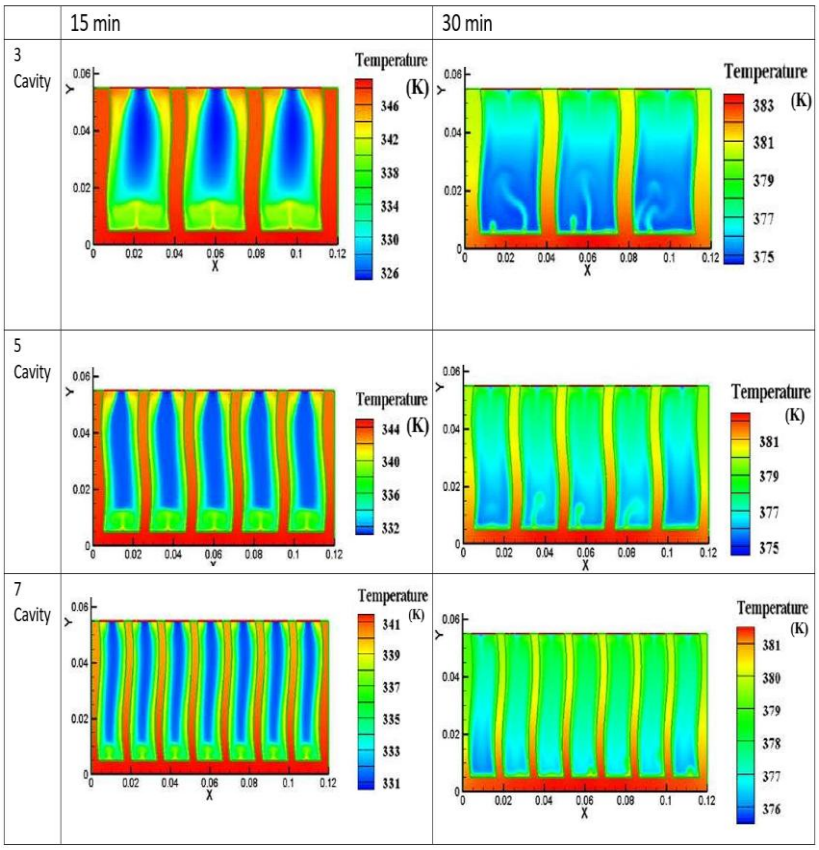


Figure 7. Temperature contours of heat sinks with different number of cavities.

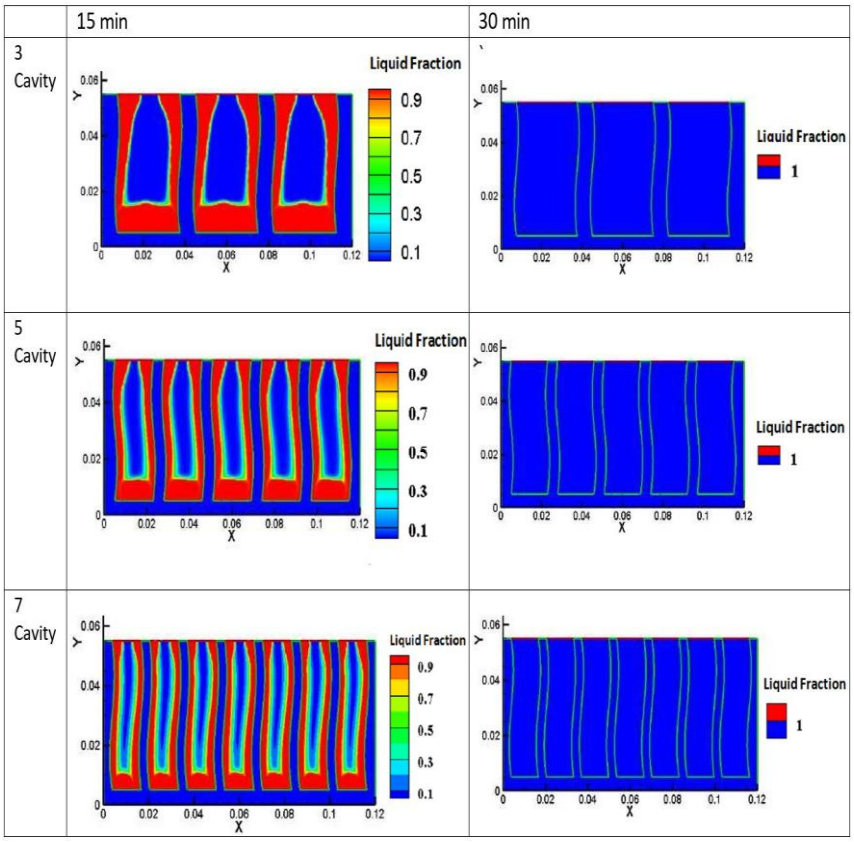
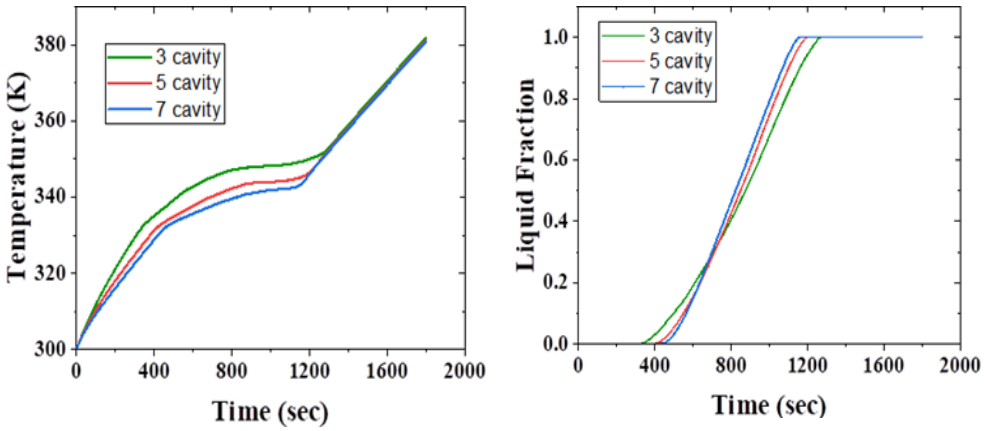


Figure 8. Liquid Fraction of heat sinks with different number of cavities.



(a) (b)

Figure 9. Graphs of heat sinks with different number of cavities. (a) Temperature variation (b) Liquid fraction.

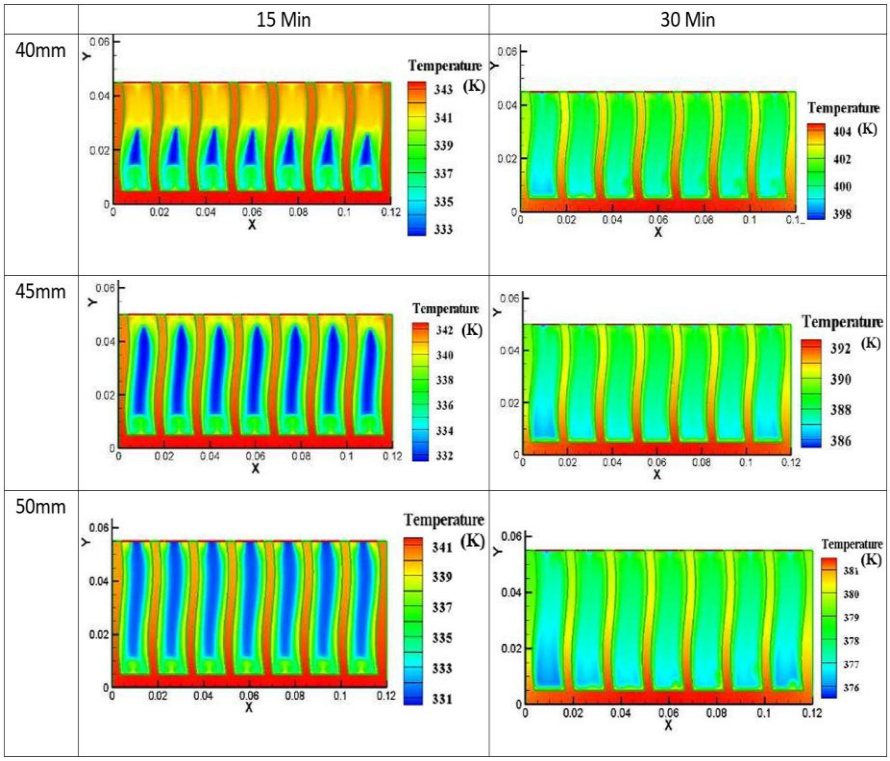


Figure 10. Temperature contour of 7 cavity heat sinks with different heights.

3.2. Comparison between heat sinks with different number of cavities

To identify the best geometry of the NePCM incorporated heat sink, the number of cavities between the fins has been varied keeping the volume of the PCM constant. The width of the wavy plate fins is also varied accordingly. The numerical simulation has been performed for 30 minutes. Figure 7 and 8 represent the Temperature and Liquid Fraction contours after 15 minutes and 30 minutes. Result shows that the heat sink with 7 number of cavities gives the best result. After 15 min and 30 min the average temperature of the 7-cavity heat sink are 340.97 K (67.81° C) and 380.78 K (107.62° C) respectively. The bottom wall temperature of the heat sink after 15 min and 30 min are 341.86 K (68.7° C) and 381.86 K (273.16° C) respectively. For 3 and 5 cavity heat sinks, the average temperature reaches 347.86 K (74.7° C) and 343.67 K (70.51° C) after 15 min and 381.72 K (108.56° C) and 381.07 K (107.91° C) after 30 min. The bottom wall temperature of the 3-cavity heat sink is 348.87 K (75.71° C) after 15 min and 382.88 K (109.72° C) after 30 min. For the 5-cavity heat sink the bottom wall of the sink attains a temperature of 344.58 K (71.42° C) and 382.17 K (109.01° C) after 15 min and

30 min respectively. Figure 9 represents the temperature and liquid fraction variation with time in heat sinks with different number of cavities. The 7-cavity heat sink performs better because of the increased contact area between the fins and the NePCM. Hence, melt fraction of PCM increases for the same time duration as compared to heat sinks with lesser number of cavities, which absorbs more latent heat. The heat sink with 7 cavities can provide more heat to the PCM for melting resulting the heat removal capacity of the 7-cavity heat sink is better.

3.3. Comparison between 7 cavity heat sinks with different heights

From the above simulations, it can be seen that the 7 cavity heat sinks are giving best results. To study the effect of the height of fins (HF), the height of the 7 cavity heat sink is varied with 40 mm, 45 mm and 50 mm values. Figure 10 and Figure 11 represent the temperature and liquid fraction contours of the different heat sinks after 15 min and 30 min.

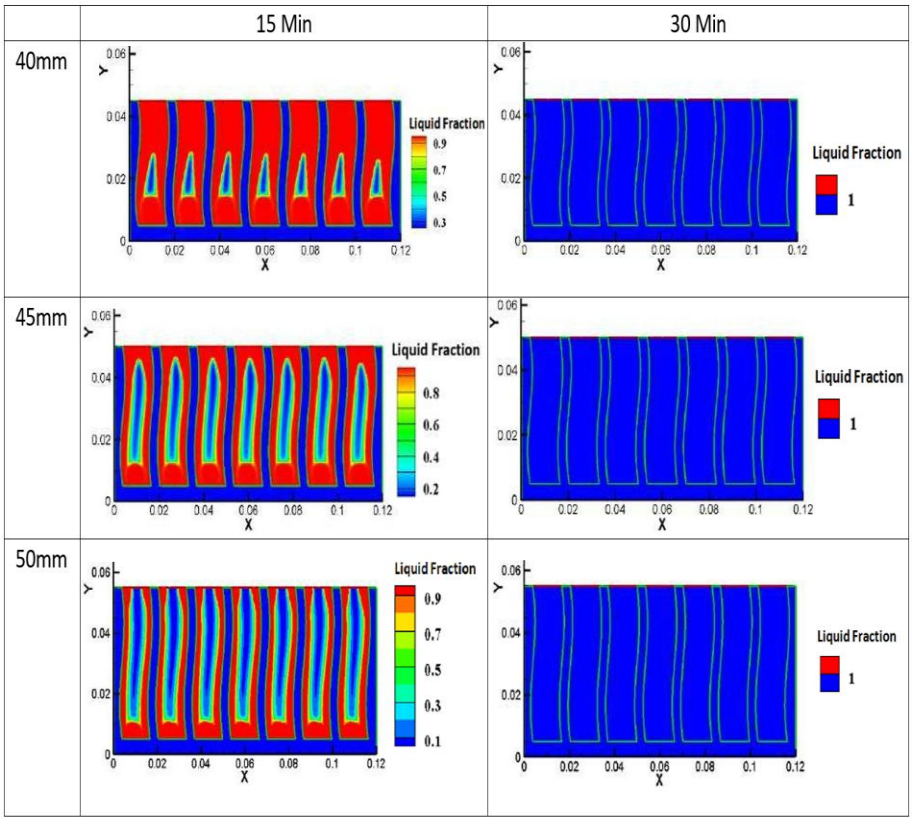
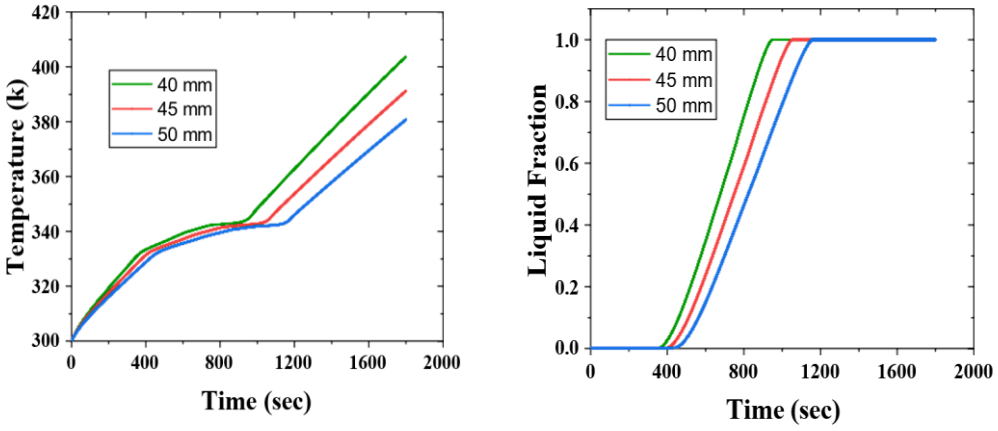


Figure 11. Liquid Fraction contour of 7 cavity heat sinks with different heights.



(a) (b)

Figure 13. Graphs of 7 cavity heat sinks with different heights (a) Temperature variation (b) Liquid fraction.

Results show that the average temperature of the heat sink with 50 mm height after 15 min and 30 min are 340.97 K (67.81° C) and 380.78 K respectively. The bottom wall temperature after 15 min and 30 min are 341.86 K (68.7°C) and 381.86 K (108.7°C) respectively. Figure 12(a) shows the temperature vs time plot for the different height heat sinks. From the graph it can be clearly seen that the heat sink with maximum height (50 mm) attains a much lower temperature than the other heat sinks for the whole simulation time. The average temperature and bottom wall temperature of the 40 mm height heat sink was 343.27 K (70.11° C) and 343.9 K (70.74° C) after 15 min and 403.77 K (130.61° C) and 404.61k (131.45°C) after 30 min. For the 45mm height heat sink the average temperature after 15 min and 30 min was 342.19 K (69.03° C) and 391.24 K (118.08° C) respectively and bottom wall temperature was 342.99 K (69.83° C) and 392.21K (119.05°C) respectively.

Figure 12(b) shows the liquid fraction variation with time for the different height heat sinks. The heat sink with maximum height is giving the best result because in that heat sink the volume of PCM is more and the surface contact area between the PCM and the fins are also more. Due to this dual advantage, the PCM between the fins absorbs the heat faster and also capable of storing more heat. That's why the heat sink with maximum height is capable of keeping the system temperature less than that of the other heat sinks for all the time as indicated from the temperature vs time curve.

4. Conclusions

This study numerically investigated the thermal performance of a nano-enhanced PCM heat sink incorporating wavy-shaped plate fins under constant heat flux conditions. The results demonstrate that the integration of NePCM significantly improves thermal management performance compared to conventional heat sinks, reducing peak temperature from 438 K to 381 K after 30 minutes. The wavy fin geometry plays a critical role by enhancing natural convection within the molten PCM, leading to faster melting and improved heat dissipation. Increasing the number of cavities from 3 to 7 resulted in improved thermal performance, reducing temperature by approximately 5–7 K due to increased contact area and enhanced heat transfer. Additionally, increasing fin height to 50 mm further improved cooling efficiency by increasing PCM volume and heat absorption capacity. Despite these improvements, the study assumes constant thermophysical properties and neglects volume expansion during phase change, which may affect accuracy. Future work should consider three-dimensional modeling and experimental validation to further assess the effectiveness of wavy fin geometries in practical applications.

References

[1] R. Viswanath, V. Wakharkar, A. Watwe, and V. Lebonheur, "Thermal performance challenges from silicon to systems," *Intel Technol. J.*, vol. 4, no. 3, pp. 1–16, 2000.

[2] D. Kraus and A. Bar-Cohen, *Thermal Analysis and Control of Electronic Equipment*. New York, NY, USA: McGraw-Hill, 1983.

[3] H. M. Ali and A. Arshad, "Experimental investigation of n-eicosane based circular pin-fin heat sinks for passive cooling of electronic devices," *Int. J. Heat Mass Transf.*, vol. 112, pp. 649–661, 2017, doi: 10.1016/j.ijheatmasstransfer.2017.05.004.

[4] G. L. Liu and J. Liu, "Convective cooling of compact electronic devices via liquid metals with low melting points," *J. Heat Transf.*, vol. 143, no. 5, Art. no. 050801, 2021, doi: 10.1115/1.4050404.

[5] A. Radwan, S. Ookawara, S. Mori, and M. Ahmed, "Uniform cooling for concentrator photovoltaic cells and electronic chips by forced convective boiling in 3D-printed monolithic double-layer microchannel heat sink," *Energy Convers. Manag.*, vol. 166, pp. 356–371, 2018, doi: 10.1016/j.enconman.2018.04.037.

[6] A. Moradikazerouni *et al.*, "Comparison of the effect of five different entrance channel shapes of a micro-channel heat sink in forced convection with application to cooling a supercomputer circuit board," *Appl. Therm. Eng.*, vol. 150, pp. 1078–1089, 2019, doi: 10.1016/j.applthermaleng.2019.01.051.

[7] S. W. Pua, K. S. Ong, K. C. Lai, and M. S. Naghavi, "Natural and forced convection heat transfer coefficients of various finned heat sinks for miniature electronic systems," *Proc. Inst. Mech. Eng. A*, vol. 233, no. 2, pp. 249–261, 2019, doi: 10.1177/0957650918784420.

[8] R. S. Kumar and S. Jayavel, "Forced convective air-cooling effect on electronic components of different geometries and orientations at flow shedding region," *IEEE Trans. Compon. Packag. Manuf. Technol.*, vol. 8, no. 4, pp. 597–605, 2018, doi: 10.1109/TCPMT.2018.2797185.

[9] K. Liang, Z. Li, M. Chen, and H. Jiang, "Comparisons between heat pipe, thermoelectric system, and vapour compression refrigeration system for electronics cooling," *Appl. Therm. Eng.*, vol. 146, pp. 260–267, 2019, doi: 10.1016/j.applthermaleng.2018.09.120.

[10] T. D. Swanson and G. C. Birur, "NASA thermal control technologies for robotic spacecraft," *Appl. Therm. Eng.*, vol. 23, no. 9, pp. 1055–1065, 2003, doi: 10.1016/S1359-4311(03)00036-X.

[11] M. Alimohammadi *et al.*, "Experimental investigation of the effects of using nano/phase change materials (NPCM) as coolant of electronic chipsets under free and forced convection," *Appl. Therm. Eng.*, vol. 111, pp. 271–279, 2017, doi: 10.1016/j.applthermaleng.2016.09.028.

[12] Y. Lv *et al.*, "A novel nanosilica-enhanced phase change material with anti-leakage and anti-volume-change properties for battery thermal management," *Energy Convers. Manag.*, vol. 163, pp. 250–259, 2018, doi: 10.1016/j.enconman.2018.02.061.

[13] R. Baby and C. Balaji, "Thermal performance of a PCM heat sink under different heat loads: An experimental study," *Int. J. Therm. Sci.*, vol. 79, pp. 240–249, 2014, doi: 10.1016/j.ijthermalsci.2013.12.018.
[14] A. Kurhade *et al.*, "Computational study of PCM cooling for electronic circuit of smartphone," *Mater. Today Proc.*, vol. 47, pp. 3171–3176, 2021, doi: 10.1016/j.matpr.2021.06.284.
[15] T. J. Lu, "Thermal management of high-power electronics with phase change cooling," *Int. J. Heat Mass Transf.*, vol. 43, no. 13, pp. 2245–2256, 2000, doi: 10.1016/S0017-9310(99)00318-X.
[16] S. Krishnan and S. V. Garimella, "Thermal management of transient power spikes in electronics: Phase change energy storage or copper heat sinks?" *J. Electron. Packag.*, vol. 126, no. 3, pp. 308–316, 2004, doi: 10.1115/1.1772411.
[17] F. L. Tan and C. P. Tso, "Cooling of mobile electronic devices using phase change materials," *Appl. Therm. Eng.*, vol. 24, no. 2–3, pp. 159–169, 2004, doi: 10.1016/j.applthermaleng.2003.09.005.
[18] R. Baby and C. Balaji, "Thermal optimization of PCM based pin fin heat sinks: An experimental study," *Appl. Therm. Eng.*, vol. 54, no. 1, pp. 65–77, 2013, doi: 10.1016/j.applthermaleng.2012.10.056.
[19] R. Kalbasi, "Introducing a novel heat sink comprising PCM and air adapted to electronic device thermal management," *Int. J. Heat Mass Transf.*, vol. 169, p. 120914, 2021, doi: 10.1016/j.ijheatmasstransfer.2021.120914.
[20] R. Bhuiya *et al.*, "Thermal management of phase change material integrated thermoelectric cooler with different heat sink geometries," *J. Energy Storage*, vol. 51, p. 104304, 2022, doi: 10.1016/j.est.2022.104304.
[21] Z. Deng *et al.*, "Experimental study on melting performance of phase change material-based finned heat sinks by a comprehensive evaluation," *J. Therm. Anal. Calorim.*, vol. 144, no. 3, pp. 869–882, 2021, doi: 10.1007/s10973-020-09508-y.
[22] M. Bayat, M. R. Faridzadeh, and D. Toghraie, "Investigation of finned heat sink performance with nano enhanced phase change material (NePCM)," *Therm. Sci. Eng. Prog.*, vol. 5, pp. 50–59, 2018, doi: 10.1016/j.tsep.2017.10.021.
[23] S. K. Saha, K. Srinivasan, and P. Dutta, "Studies on optimum distribution of fins in heat sinks filled with phase change materials," *J. Heat Transf.*, vol. 130, no. 3, Art. no. 034505, 2008, doi: 10.1115/1.2804948.
[24] C. Oluah, E. T. Akinlabi, and H. O. Njoku, "Selection of phase change material for improved performance of Trombe wall systems using the entropy weight and TOPSIS methodology," *Energy Build.*, vol. 217, Art. no. 109967, 2020, doi: 10.1016/j.enbuild.2020.109967.
[25] A. Kumar, R. Kothari, S. K. Sahu, and S. I. Kundalwal, "Thermal performance of heat sink using nano-enhanced phase change material (NePCM) for cooling of electronic components," *Microelectron. Reliab.*, vol. 121, Art. no. 114144, 2021, doi: 10.1016/j.microrel.2021.114144.
[26] H. Bashirpour-Bonab, "Investigation and optimization of PCM melting with nanoparticle in a multi-tube thermal energy storage system," *Case Stud. Therm. Eng.*, vol. 28, p. 101643, 2021, doi: 10.1016/j.csite.2021.101643.
[27] N. Pradeep *et al.*, "Silver nanoparticles for enhanced thermal energy storage of phase change materials," *Mater. Today Proc.*, vol. 45, pp. 607–611, 2021, doi: 10.1016/j.matpr.2020.02.671.
[28] K. Chopra *et al.*, "Effect of simultaneous and consecutive melting/solidification of phase change material on domestic solar water heating system," *Renew. Energy*, vol. 188, pp. 329–348, 2022, doi: 10.1016/j.renene.2022.01.059.
[29] P. M. J. Stalin *et al.*, "Investigations on thermal properties of CeO_2/water nanofluids for heat transfer applications," *Mater. Today Proc.*, vol. 47, pp. 6815–6820, 2021, doi: 10.1016/j.matpr.2021.05.137.
[30] V. Shatikian, G. Ziskind, and R. Letan, "Numerical investigation of a PCM-based heat sink with internal fins," *Int. J. Heat Mass Transf.*, vol. 48, no. 17, pp. 3689–3706, 2005, doi: 10.1016/j.ijheatmasstransfer.2004.10.042.
[31] V. Shatikian *et al.*, "Simulation of PCM melting and solidification in a partitioned storage unit," in *Proc. Heat Transfer Summer Conf.*, vol. 36940, pp. 347–353, Jan. 2003, doi: 10.1115/HT2003-47167.
[32] S. L. Tariq *et al.*, "Nanoparticles enhanced phase change materials (NePCMs): A recent review," *Appl. Therm. Eng.*, vol. 176, p. 115305, 2020, doi: 10.1016/j.applthermaleng.2020.115305.
[33] H. Yang, Y. Li, L. Zhang, and Y. Zhu, "Thermal performance enhancement of phase change material heat sinks for thermal management of electronic devices under constant and intermittent power loads," *Int. J. Heat Mass Transf.*, vol. 181, p. 121899, 2021, doi: 10.1016/j.ijheatmasstransfer.2021.121899.
[34] T. Ramesh, A. S. Praveen, P. B. Pillai, and S. Salunkhe, "Phase change material aided thermal scheming of high-power LED: Effect of PCM with varying pitch of hexagonal fins," *Mater. Res. Innov.*, vol. 26, no. 6, pp. 331–340, 2022, doi: 10.1080/14328917.2021.1984665.
[35] H. Nazir *et al.*, "Recent developments in phase change materials for energy storage applications: A review," *Int. J. Heat Mass Transf.*, vol. 129, pp. 491–523, 2019, doi: 10.1016/j.ijheatmasstransfer.2018.09.126.
[36] M. Mozafari, A. Lee, and J. Mohammadpour, "Thermal management of single and multiple PCMs based heat sinks for electronics cooling," *Therm. Sci. Eng. Prog.*, vol. 23, p. 100919, 2021, doi: 10.1016/j.tsep.2021.100919.
[37] M. Mohammadi, A. Taheri, M. Passandideh-Fard, and M. Sardarabadi, "Electronic chipset thermal management using a nanofluid-based mini-channel heat sink: An experimental study," *Int. Commun. Heat Mass Transf.*, vol. 118, p. 104836, 2020, doi: 10.1016/j.icheatmasstransfer.2020.104836.
[38] S. Mahmoud *et al.*, "Experimental investigation of inserts configurations and PCM type on the thermal performance of PCM based heat sinks," *Appl. Energy*, vol. 112, pp. 1349–1356, 2013, doi: 10.1016/j.apenergy.2013.04.059.
[39] Y. Kozak, B. Abramzon, and G. Ziskind, "Experimental and numerical investigation of a hybrid PCM-air heat sink," *Appl. Therm. Eng.*, vol. 59, no. 1–2, pp. 142–152, 2013, doi: 10.1016/j.applthermaleng.2013.05.021.
[40] A. Arshad *et al.*, "An experimental study of enhanced heat sinks for thermal management using n-eicosane as phase change material," *Appl. Therm. Eng.*, vol. 132, pp. 52–66, 2018, doi: 10.1016/j.applthermaleng.2017.12.066.
[41] X. Q. Wang, C. Yap, and A. S. Mujumdar, "A parametric study of phase change material (PCM)-based heat sinks," *Int. J. Therm. Sci.*, vol. 47, no. 8, pp. 1055–1068, 2008, doi: 10.1016/j.ijthermalsci.2007.07.016.
[42] B. Kamkari and D. Groulx, "Experimental investigation of melting behaviour of phase change material in finned rectangular enclosures under different inclination angles," *Exp. Therm. Fluid Sci.*, vol. 97, pp. 94–108, 2018, doi: 10.1016/j.expthermflusci.2018.04.007.
[43] R. Karami and B. Kamkari, "Investigation of the effect of inclination angle on the melting enhancement of phase change material in finned latent heat thermal storage units," *Appl. Therm. Eng.*, vol. 146, pp. 45–60, 2019, doi: 10.1016/j.applthermaleng.2018.09.105.